AKAP-PKA interactions regulate airway smooth muscle contractility and proliferation

Bing Han[1,2], Wilfred J. Poppinga[1,2], Saskia Driessen[1], Carolina R.S. Elzinga[1], Andrew J. Halayko[3], Herman Meurs[1,2], Harm Maarsingh[4], M. Schmidt[1,2]

[1] University of Groningen, Department of Molecular Pharmacology, Groningen, The Netherlands;
[2] GRIAC research institute, University of Groningen, University Medical Center Groningen, The Netherlands;
[3] Department of Physiology and Pathophysiology, University of Manitoba, Winnipeg, Manitoba, Canada.
[4] Palm Beach Atlantic University, Lloyd L. Gregory School of

3

Abstract

With the ability of switching between a proliferative and a contractile phenotype, airway smooth muscle (ASM) cells play an important role in the progression of airway diseases such as asthma and chronic obstructive pulmonary disease (COPD). This capacity underpins, in part, airway remodeling in asthma as well as COPD, with patients very often exhibiting ASM hypertrophy associated with hypercontractility. A-kinase anchoring proteins (AKAPs) provide a molecular platform to ensure that signaling effectors are appropriately targeted to facilitate intracellular signal transduction. A unifying feature of AKAPs is their ability to anchor protein kinase A (PKA) in proximity to its substrates near membrane structures. Several studies indicate that interruption of AKAP-PKA function leads to cellular dysfunction. As stearated (st)-Ht31, a peptide that disrupts the interaction of AKAP and PKA, affects a variety of cellular functions, including cardiac muscle contraction and cell cycle progression, we studied here whether st-Ht31 alters airway smooth muscle function. We report that treatment of ASM cells with st-Ht31 enhances proliferative markers such as DNA synthesis, cyclin D expression as well as phosphorylation of retinoblastoma protein and p70S6 kinase, a process accompanied by a downregulation of AKAP8. Interestingly, st-Ht31 also promotes accumulation of contractile marker proteins, including α-smooth muscle actin (SMA) and calponin, presumably by regulating protein stability. Of note, treating intact human ASM strips with st-Ht31 simultaneously enhanced α-SMA abundance and muscle contraction, whilst concomitantly increasing abundance of the S phase marker proliferating cell nuclear antigen.

Taken together, treating ASM with st-Ht31 leads to a simultaneous increase in markers of both a hypercontractile and a hyperproliferative phenotype in both ASM cells and intact ASM strips. Thus, AKAP-PKA interaction could play a critical role to maintain ASM normal function, therefore preventing progression of airways diseases such as asthma and COPD.

Introduction

Airway smooth muscle (ASM) cells have capacity for phenotypic plasticity and are able to switch between a more proliferative (and less contractile) or a more contractile (and less proliferative) phenotype in response to microenvironment changes in mitogens, growth factors such as transforming growth factor-β, and extracellular matrix composition (Halayko et al. 2008). Phenotypic plasticity of ASM plays an important role in the pathophysiology of obstructive pulmonary diseases, such as chronic obstructive pulmonary disease (COPD) and asthma, by enabling airway hypercontractility and increased ASM mass (Halayko et al. 2008), which contribute to airway narrowing and airflow limitation (Amrani and Panettieri 2003; Chung 2005). The hypercontractile phenotype is characterized by an increased expression of contractile proteins, such as α-smooth muscle actin (SMA) and calponin (Halayko et al. 2008). We have shown that cAMP regulates mitogen-induced phenotypic plasticity (Roscioni et al. 2011a; Roscioni et al. 2011c) and that activation of the cAMP effector protein kinase A (PKA) both prevents mitogen-induced proliferation by blunting the activation of ERK and p70S6K, as well as inhibiting mitogen-induced reduction in contractile protein expression in ASM strips (Roscioni 2011 and 2011).

A-kinase anchoring proteins (AKAPs) are scaffolding proteins that provide a molecular platform for other proteins to ensure that signaling effectors are appropriately targeted to different domains, thereby specifying and facilitating intracellular signal transduction (Wong and Scott 2004). Several AKAP isoforms have been identified that can differ in their cellular localization (Skroblin et al. 2010). A unifying feature of AKAPs is their ability to anchor the regulatory subunits of PKA in proximity to substrates via a conserved short α helical structure (Esseltine and Scott 2013). Besides PKA, each AKAP can bind several receptors, ion channels, protein kinases, phosphatases, small GTPases and phosphodiesterases to orchestrate formation of unique signaling complexes (Poppinga et al. 2014; Han et al. 2015). AKAPs are important in compartmentalizing cAMP within the cellular context, thus providing spatio-temporal regulation of the cAMP pathway (Wong and Scott 2004). On this basis, AKAPs regulate a number of cellular responses including intracellular actin dynamics (Kim et al. 2013) and cell cycle progression (Han et al. 2015). All AKAPs bind to the regulatory subunits of PKA through a conserved short α helical structure (Pawson and Scott 1997), and based here on a cell permeable inhibitor peptide, stearated (st)-Ht31, was developed to block the interaction between all members of the AKAP family and PKA (Vijayaraghavan et al. 1997; Poppinga et al. 2014).

Cell cycle kinetics is controlled by various effectors, including p70S6 kinase (p70S6K), extracellular signal-regulated kinase (ERK), proliferating cell nuclear antigen (PCNA), cyclins, and retinoblastoma protein (Rb) (Leonardi et al. 1992; Karpova et al. 1997; Grewe et al. 1999; Bertoli et al. 2013; Dick and Rubin 2013). Of note, most of these effectors can interact with AKAPs (Han et al. 2015), and dysfunction of AKAPs is associated with cell cycle dysregulation

(Akakura et al. 2008; Pellagatti et al. 2010; Kong et al. 2013; Petrilli and Fernández-Valle 2015). A number of AKAPs have been identified in ASM, including AKAP8 (aka AKAP95) (Horvat et al. 2012; Poppinga et al. 2015), which can interact with cyclin D1 (Arsenijevic et al. 2004). However, the a more general role for AKAPs in regulating cell cycle transit and contractility in ASM is yet to be defined. Using a unique a specific AKAP-PKA interaction disruptor, st-Ht31 (Skroblin et al. 2010), the current study explores the role of AKAPs in regulating airway smooth muscle contractility and proliferation.

Methods

Cell culture

Human ASM cell cultures were generated from macroscopically healthy 3rd-5th generation bronchial segments obtained from three different donors undergoing lung resection surgery, and thereafter low passage number primary cultures (P2-P3) were made senescence-resistant by stable ectopic expression of human telomerase reverse transcriptase (hTERT) as described previously (Gosens et al. 2006). Cell cultures were maintained in DMEM (Life technologies, 11965-092) containing heat-inactivated fetal bovine serum (10% vol/vol), streptomycin (50 U/ml) and penicillin (50 mg/ml) in a humidified atmosphere at 37 °C in air/CO_2 (95%:5% vol/vol). hTERT ASM cultures up to passage 30 were used.

[^{3}H]-Thymidine incorporation assay

hTERT ASM cells were plated in 24-well plates at 20,000 cells/well. After growing to confluence, cells were serum deprived for 3 days and subsequently incubated with 50 μM st-Ht31 (V8211, Promega) or vehicle for 4 h, then incubated in the presence of [^{3}H]-thymidine (0.25 μCi·ml^{-1}) for 24hr. After incubation, cells were washed twice with PBS at room temperature and subsequently with ice-cold 5% trichloroacetic acid on ice for 30 min and the acid-insoluble fraction was dissolved in 1 ml NaOH (1 M). Incorporated [^{3}H]-thymidine was quantified by liquid-scintillation counting using a Beckam LS1701 β-counter as described previously (Roscioni et al. 2011a).

Cell proliferation assay

hTERT ASM cells were plated in 24-well plates at 20,000 cells/well and serum deprived for 3 days. After incubation with 50 μM st-Ht31 or vehicle for 4 days, cells were washed twice with PBS and incubated with a 5% vol/vol AlamarBlue® (DAL1100, Thermo Fisher) in HBSS for about 45 min. AlamarBlue® is converted into its fluorescent form by mitochondrial cytochromes in viable cells. Therefore, the amount of fluorescence is proportional to the number of living cells. Proliferation was assessed by measuring fluorescence emission using a Wallac 1420 Victor 2TM (excitation: 570 nm, emission: 590 nm).

Fluorescence-activated cell sorting analysis

To study the effect of st-Ht31 on cell cycle distribution, fluorescence-activated cell sorting (FACS) analysis was performed in the hTERT ASM cells. hTERT ASM cells were plated in 6-well plates at a concentration of 200,000 cells/well. After growing to confluence, cells were serum deprived for 3 days and subsequently treated with 50 µM st-Ht31 or vehicle for 24 h. After incubation, cells were detached by trypsin treatment and washed twice with warm PBS (37°C). Cells were then resuspended in ice-cold PBS and fixed by transferring into ice-cold 70% ethanol. After centrifugation, the cell pellet was resuspended in PBS containing 10 µg/ml propidium iodide, 20 mM EDTA, 0.05% Tween 20 and 50 µg/ml RNAse, and incubated at 4°C overnight. Cell cycle analysis was performed on a BD FACSCalibur (Becton, Dickinson and Company, BD, Franklin Lakes, NJ, USA). Fluorescence histograms were collected for at least 10,000 cells. The cell cycle distribution was analyzed using ModFit LT flow cytometry modelling software (ModFit LT, version 4.0.5).

Western blot

hTERT ASM cells were plated in 6-well plates at a concentration of 200,000 cells/well. After serum deprivation for 3 days, cells were treated with 50 µM st-Ht31 for 24 h. For α-SMA and calponin expression, cells were serum deprived for 1 day, followed by a 4 day treatment with 50 µM st-Ht31. To study the possible mechanisms of st-Ht31 on α-SMA and calponin protein expressions, inhibitors (MG-132: 5 µM, ab141003, Abcam; cycloheximide: 5 mg/ml, 44189, BDH Biochemicals; actinomycin D: 1 µg/ml, A1410, Sigma; chloroquine diphosphate salt: 50 µM, C6628, Sigma) were added for the final 24 h. After washing twice with ice-cold PBS, cells were lysed using 100 µl of RIPA buffer (composition: 50 mM Tris, 150 mM NaCl, 0.1% SDS, 0.5% sodium deoxycholate, 1% nonyl phenoxypolyethoxylethanol), supplemented with 1 mM Na_3VO_4, 1 mM NaF, 1,06 mg/ml β-glycerolphosphate, 1 µg/ml apoprotein, 1 µg/ml leupeptin, and 1 µg/ml pepstatin A. The cell lysate was homogenized by passing through a 25-gauge needle for 10 times. Protein content was determined using the Pierce BCA protein assay.

Equal amounts of protein were prepared for SDS-PAGE by adding 4X SDS loading buffer and ultrapure water, and separated on a 10% polyacrylamide gel and transferred to a nitrocellulose membrane, followed by blocking with 1x Roti®-Block (A151, Carl Roth), and incubated overnight with primary antibodies (see Table 1). After washing, the membranes were incubated with horseradish peroxidase-labelled secondary antibodies (see Table 1). Protein bands were visualized using Western Lightning® Plus-ECL (NEL104001EA, PerkinElmer) and quantified using ImageJ J 1.48v. Proteins were normalized to GAPDH, lamin AC or caveolin-1. These protein expressions were found unaltered under the experimental conditions (data not shown).

Table 1. Antibodies used for Western blot analysis

Protein of interest	Primary antibody	Secondary antibody
α-SMA	1:1000, A2547, Sigma	1:2000, A9044, Sigma
Calponin	1:1000, C2687, Sigma	1:5000, A9044, Sigma
PCNA	1:1000, sc-7907, Santa-Cruz	1:2000, A0545, Sigma
Pan-ubiquitin	1:1000, ab7780, Abcam	1:3000, A0545, Sigma
Cyclin D1	1:1000, #2926, Cell Signaling	1:1000, A9044, Sigma
Phosphorylated (p)-Rb	1:500, #9308, Cell Signaling	1:1000, A0545, Sigma
p-p70S6K	1:500, sc-7984-R, Santa-Cruz	1:2000, A0545, Sigma
p-ERK	1:2000, #9101S, Cell Signaling	1:5000, A0545, Sigma
Caveolin-1	1:1000, sc-894 (HRP conjugated), Santa-Cruz	Not necessary
Lamin AC	1:1000, sc-7292, Santa-Cruz	1:2000, A9044, Sigma
GAPDH	1:2000, sc-47724, Santa-Cruz	1:8000,A9044, Sigma

Co-immunoprecipitation

For co-immunopreciptation (Co-IP), hTERT ASM cells were plated in 10 cm dishes. After grown to confluence, cells were serum deprived for 1 day and subsequently treated with 50 μM st-Ht31 or vehicle for 4 days. After treatment, cells were lysed using Co-IP buffer (composition: 40 mM HEPES, 120 mM NaCl, 0.5% Triton-X-100, 10% glycerol and 1 mM EDTA), supplemented with 1 mM Na3VO4, 1 mM NaF, 1,06 mg/ml β-glycerolphosphate, 1 μg/ml apoprotein, 1 μg/ml leupeptin and 1 μg/ml pepstatin A. Protein content was determined using the Pierce BCA protein assay. Equal amounts of protein (1 mg) were distributed in 2 incubation tubes. 2 μg anti-α-SMA (A2547, Sigma) or normal mouse IgG (used as control IgG, SC-2025, Santa-Cruz) were added to the cell lysates to incubate overnight at 4 ºC. Then, 50 μl protein A/G PLUS-Agarose beads (sc-2003, Santa-Cruz) were added per incubation tube and incubated for 4 h at 4 ºC. After washing for 5 times with Co-IP buffer, beads were resuspended in 25 μl 4X SDS loading buffer and 25 μl Co-IP buffer. The degree of ubiquitination of proteins was detected using western blot analysis (see above for technical details).

Immunofluorescence

hTERT ASM cells were plated at a density of 20,000 cells per well on a 24-well plate with cover slips placed at the bottom of each well. For α-SMA expression, cells were serum deprived for 1 day and subsequently treated with 50 μM st-Ht31 or vehicle for 4 days. For cyclin D1 and AKAP8, cells were serum deprived for 3 days and subsequently treated with 50 μM st-Ht31 or vehicle for 24 h. After stimulation, cells were washed twice with PBS and fixed with 4% paraformaldehyde + 4% sucrose for 15 min, followed by 0.3% Triton X100 for 2 min at room

temperature. Cells were then blocked with a blocking buffer containing 5% bovine serum albumin (BSA) and 2% donkey serum at room temperature for 1 h. After fixing, cells were incubated overnight at 4°C with the primary antibody (α-SMA: 1:1000, A2547, Sigma; cyclin D1: 1:100, #2926, Cell Signaling; AKAP8: 1:50, sc-10766, Santa-Cruz) diluted in 1% BSA. The next day, after through wash, cells were incubated with the secondary antibody (anti-rabbit FITC, Green, 1:500, 65-6111, ThermoFisher) for 1 h at room temperature in a dark chamber. After a thorough wash, nuclei were stained with Hoechst (1:10,000, H3570, Invitrogen) for 5–10 s, immediately followed by two quick and four 10-min washing steps with dd-H_2O. Finally, cover slips were placed and attached on microscope slides using ProLong Gold antifade reagent (Invitrogen). Images were taken and analyzed using an Olympus AX70 microscope equipped with digital image capture system (ColorView Soft System with Olympus U CMAD2 lens, Olympus Corporation, Tokyo, Japan). The background corrected fluorescence measurements were performed with Image J 1.48v (Burgess et al. 2010).

mRNA isolation and real time PCR

hTERT ASM cells were plated in 6-well plates at a concentration of 200,000 cells/well. After serum deprivation [1 day for actin alpha 2 (Acta2), calponin 1 (Cnn1), and 3 days for AKAP8], cells were treated with 50 μM st-Ht31 for 10 h. mRNA from hTERT ASM cells was extracted using a Nucleospin RNA II kit (Machery Nagel) and quantified using spectrophotometry (Nanodrop, ThermoScientific). 1 μg of mRNA was converted in cDNA by reverse transcriptase using Promega tools (Madison). cDNA was subjected to real-time PCR (RT-PCR) using a MyiQ™ Single-Color detection system (Bio-Rad Laboratories Inc. Life Science Group) and the specific primers (see Table 2). RT-qPCR was performed in duplicate using SYBR Green (Roche) with denaturation at 94 °C for 30 s, annealing at 59°C for 30 s and extension at 72°C for 30 s for 40 cycles followed by 10 min at 72 °C. The amount of target gene was normalized to ribosomal subunit 18 S (designated as ΔCT). Relative differences were determined using the equation $2^{-(\Delta\Delta Ct)}$.

Table 2. Primers used for RT-PCR

Gene of interest	Primers
Acta2	Forward 5′-CTTTCATTGGGATGGAGTCAGC-3′
	Reverse 5′-ACAGGACGTTGTTAGCATAGAGA-3′
Cnn2	Forward 5′-TCTTTGAGGCCAACGACCTG-3′
	Reverse 5′-GGGATCATAGAGGTGACGCC-3′
AKAP8	Forward 5′-ATGCACCGACAATTCCGACT-3′
	Reverse 5′-CATAGGACTCGAACGGCTGG-3′
18S	Forward 5′-CGCCGCTAGAGGTGAAATTC-3′
	Reverse 5′-TTGGCAAATGCTTTCGCTC-3′

Human tracheal smooth muscle strips

Human tracheal tissue from anonymized lung transplantation donors was obtained from the Department of Cardiothoracic Surgery, University Medical Center Groningen. After dissection of the smooth muscle layer and careful removal of the mucosa and connective tissue, human tracheal smooth muscle strips of identical length and width were prepared as described previously (Roscioni et al. 2011c). Tissue strips were transferred to serum-free DMEM supplemented with sodium pyruvate (1 mM), non-essential amino acid mixture (1:100), gentamicin (45 µg/ml), penicillin (100 U/ml), streptomycin (100 µg/ml), amphotericin B (1.5 µg/ml), apo-transferrin (human, 5 µg/ml) and ascorbic acid (100 µM). The strips were incubated with 50 µM st-Ht31 or vehicle for 4 days in an Innova 4000 incubator shaker (37 °C, 55 rpm). After culture, strips were mounted in the organ bath for isometric tension measurements.

Isometric contraction measurement

Isometric contraction experiments were performed essentially as described previously (Roscioni et al. 2011c). Briefly, ASM strips were mounted for isometric recording in 20-ml organ-baths, containing Krebs-Henseleit buffer at 37 °C. During a 90 min equilibration period with wash-outs every 30 min, resting tension was adjusted to 1 g, followed by pre-contractions with 10 µM methacholine. Following wash-out, maximal relaxation was established by the addition of 0.1 µM (-)-isoprenaline. Tension was readjusted to 1 g, followed by refreshing of the Krebs-Henseleit buffer twice. After another equilibration period of 30 min, cumulative concentration–response curves were constructed with methacholine (0.1 nM – 1 mM). When maximal tension was reached, strips were washed several times and maximal relaxation was established using 10 µM (-)-isoprenaline. Contractions were expressed as percentage of maximal contraction induced by methacholine in basal strips, corrected for tissue weight. Curves were fitted using Prism 5.0. After the contraction protocol, strips were collected and tissue homogenates were prepared as previously described (Roscioni et al. 2011c) for western blot measurement of α-SMA, calponin and PCNA.

Statistics

Data are expressed as means ± SEM of *n* individual experiments. Statistical significance of differences was evaluated by paired two tailed Student's t-test using Prism 5 software. Non-linear curve fit was performed in Prism 5.0, and curve comparison was done by extra sum-of-squares F test using Prism 5.0 software. Differences were considered to be statistically significant when $p<0.05$.

Results

Role of AKAPs in proliferation of ASM cells

Treatment for 1 day with st-Ht31 significantly increased [^{3}H]-thymidine incorporation in ASM cells (Figure 1A), indicating that DNA synthesis was induced. However, st-Ht31 treatment for 4 days did not increase AlamarBlue® conversion (Figure 1B), demonstrating that the early increase in DNA synthesis did not result in an increase in cell number. We further assessed cell cycle distribution of propidium iodide stained ASM cells by flow cytometry and found that st-Ht31 exposure had little effect, with only the suggestion of a small, but not statistically significant, change S phase cell number (Figure 1C).

To further understand the paradoxical increase in DNA synthesis without cell cycle induction with st-Ht31 treatment, we next investigated the abundance and phosphorylation of cell cycle regulator proteins. Western blotting revealed that 1-day treatment with st-Ht31 increased cyclin D1 abundance (Figure 1D), and this was confirmed microscopically by assessing immunofluorescence in fixed cell (Figure 1E). In addition, both Rb phosphorylation and phosphorylation of p70S6K were significantly increased in st-Ht31 treated hTERT ASM cells, whereas ERK phosphorylation was unaffected (Figures 1F-1H).

AKAP8 expression and localization in ASM cells

One day treatment with st-Ht31 decreased the fluorescent intensity of total AKAP8 in hTERT ASM cells compared to untreated cells (Figure 2A). The ratio of the distribution of AKAP8 between nuclei and cytoplasm was not altered by st-Ht31, suggesting a treatment causes a general decrease in AKAP8 abundance (Figure 2A). In line with the changes on protein level, we found that 10 h treatment with st-Ht31 also significantly decreased the AKAP8 gene expression (Figure 2B). Next to AKAP8, we also measured the expression of AKAP5, 12 and Ezrin, which were not significantly altered by st-Ht31 (data not shown).

Role of AKAPs in contractile protein expression in ASM cells

Four days of treatment with st-Ht31 induced a significant increase in both α-SMA and calponin protein in hTERT ASM cells as measured by western blot (Figure 3A). Increased α-SMA protein was also confirmed using microscopy to assess immunofluorescence of fixed cells (Figure 3C). The abundance of mRNA for *Acta2* and *Cnn1*, which encode α-SMA and calponin, respectively, was measured after 10 h of treatment with st-Ht31. Although protein abundance of α-SMA and calponin increased, the mRNA abundance for *Cnn1* was not changed, and decreased for *Acta2* (Figure 3B).

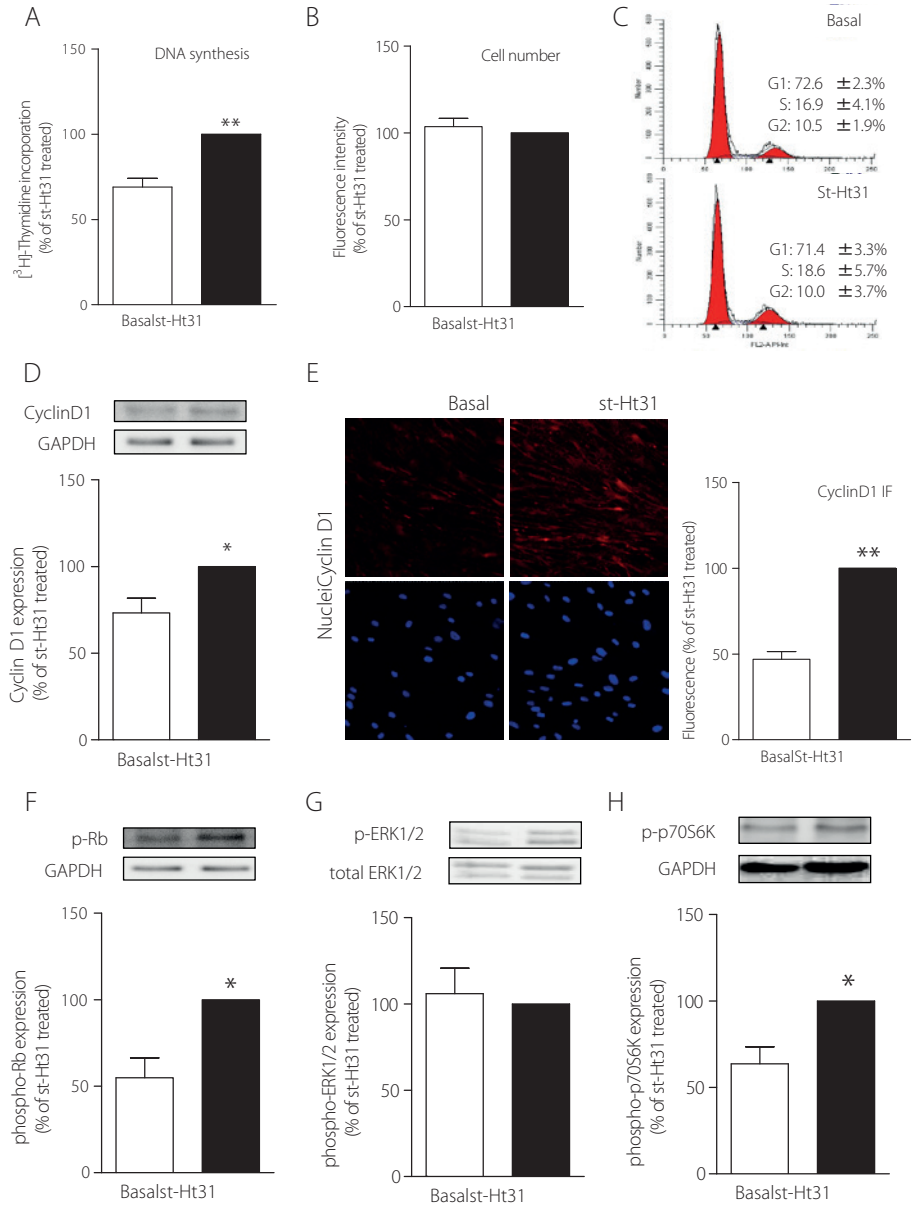

Figure 1. The effects of st-Ht31 on proliferative markers. hTERT ASM cells were serum-deprived for 3 days and treated with 50 μM st-Ht31. **A**: [3H]-thymidine was added 4 h after st-Ht31 and incorporated [3H]-thymidine was quantified 24 h later. N=15. **B**: After 4 days of treatment with st-Ht31, cell number was assessed using AlamarBlue®. N=5. **C**: FACS analysis was performed 24 h after st-Ht31 treatment. N=3. **D-H**: Protein expression of the indicated proteins was measured 24 h after st-Ht31 treatment using Western blot (D, F-H) or immunofluorescence (IF, **E**). N=4-9. *p<0.05 and **p<0.01 compared to basal (paired two tailed Student's t-test).

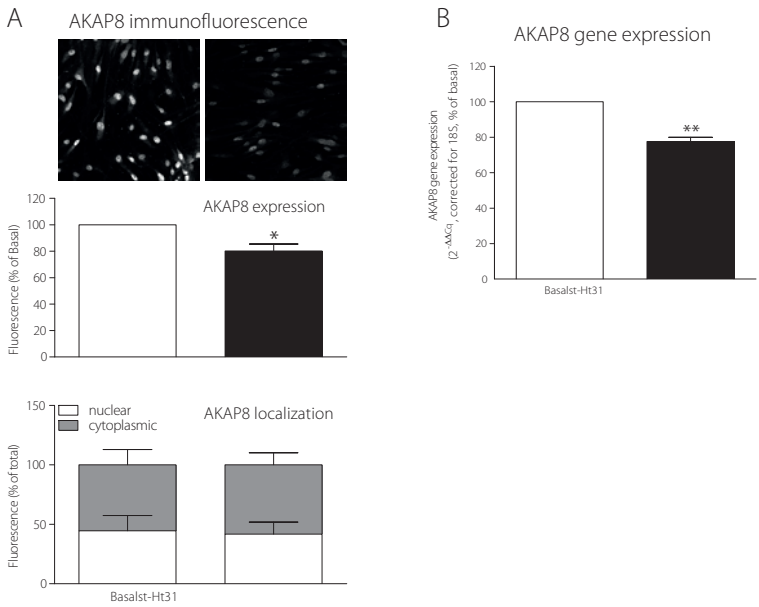

Figure 2. The effects of st-Ht31 on AKAP8 expression and cellular localization. hTERT ASM cells were serum deprived for 3 days and treated with 50 μM st-Ht31 for 24 h. **A**: The expression and localization of AKAP8 were measured by immunofluorescence. Representative images are shown. Images were quantified by Image J 1.48v. N=4, *p<0.05, two tailed Student's t-test. **B**: AKAP8 mRNA was measured using RT-PCR and normalized to ribosomal subunit 18 S (ΔCT). Relative differences were determined using the equation $2^{-(\Delta\Delta Ct)}$. N=4. *p<0.05 and **p<0.01 compared to basal (paired two tailed Student's t-test).

To investigate the underpinnings of the differences in the effects of st-Ht31 on mRNA and proteins for α-SMA and calponin, we examined the effects of a number of pharmacologic inhibitors of transcription, translation and protein degradation. Blocking RNA synthesis using actinomycin D decreased basal α-SMA and calponin protein abundance (Figure 3E, Figure 4A). The presence of actinomycin D had no impact in st-Ht31-induced accumulation of α-SMA and calponin protein (Figure 3E, Figure 4A). Similarly, blocking protein translation using cycloheximide did not significantly affect the basal expression of either α-SMA or calponin, nor did it affect st-Ht31-induced α-SMA and calponin accumulation (Figure 3E, Figure 4B). Furthermore, blocking lysosomal degradation of proteins using chloroquine had no effect on basal or st-Ht31-induced α-SMA and calponin protein abundacne (Figure 3E, Figure 4D). Interestingly, though blocking proteasomal degradation of ubiquitin-conjugated proteins using MG-132 did not affect basal α-SMA protein and increased calponin protein (Figure 3E, Figure 4C), and though st-Ht31 did increase ubiquitination of α-SMA (Figure 3D), MG-132 was without effect on the magnitude of st-Ht31 induced calponin or α-SMA protein abundance (Figure 3E, Figure 4C).

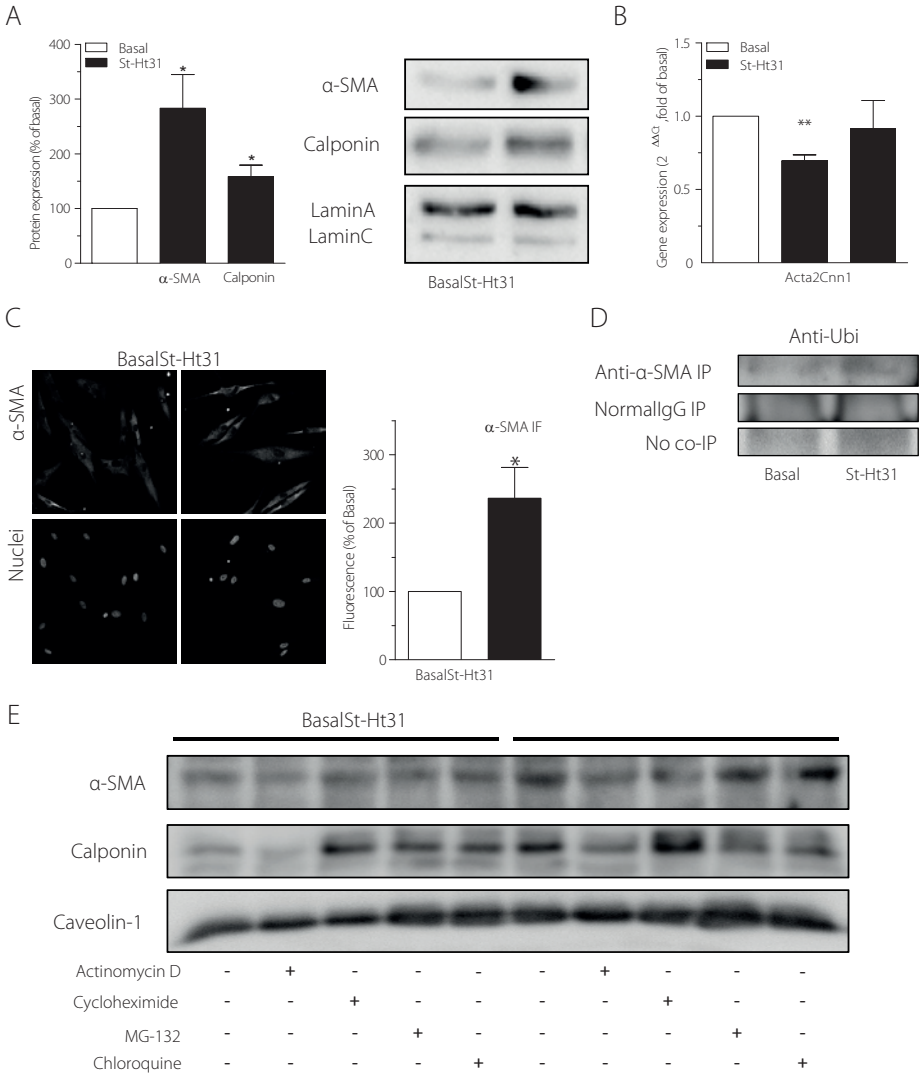

Figure 3. The effect of st-Ht3 on contractile markers. hTERT ASM cells were serum deprived for 1 day and treated with 50 μM st-Ht31 for 4 days (A, C-E) or 1 h (B). Data expressed as means ± SEM of N experiments. **A, C**: Protein expression of α-SMA (A, C) and calponin (A) were measured by western blot (A) or immunofluorescence (IF, C). N=8. **B**: Acta2 and Cnn1 mRNA expression was measured using RT-PCR and normalized to ribosomal subunit 18 S (ΔCT). Relative differences were determined using the equation $2^{-(\Delta\Delta Ct)}$. N=4. **D**: Cell lysates were first immunoprecipitated (IP) by using anti-α-SMA or normal IgG. The degree of protein ubiquitination was detected using an anti-ubiquitin (Ubi) antibody. **E**: 1 μg/ml actinomycin D, 5 mg/ml cycloheximide, 5 μM MG-132 and 50 μM chloroquine were added for the final 24 h of st-Ht31 treatment and protein expression of the indicated proteins was measured using Western blot. Representative blots are shown (quantifications are shown in Figure 4). *p<0.05 and **p<0.01 compared to basal (paired two tailed Student's t-test).

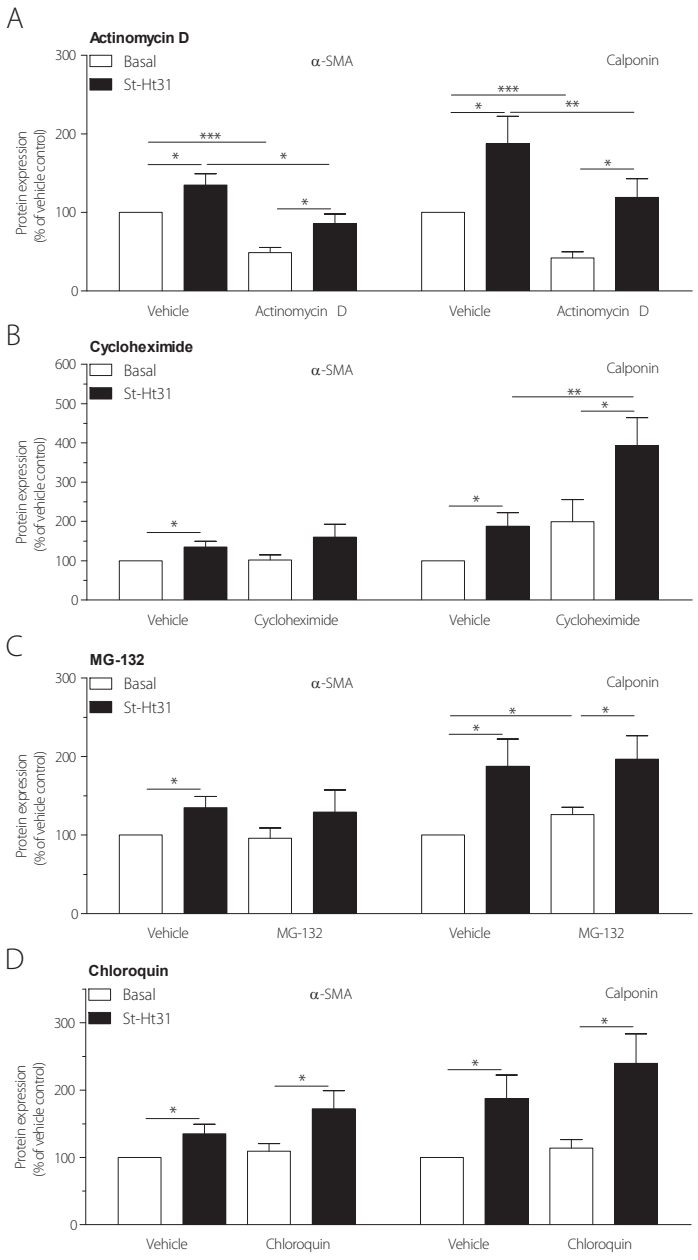

Figure 4. The involvement of post-transcriptional processes in the effect of st-Ht31 on α-SMA and calponin protein expression. hTERT ASM cells were serum deprived for 1 day and treated with 50 μM st-Ht31 for 4 days. 1 μg/ml actinomycin D (**A**), 5 mg/ml cycloheximide (**B**), 5 μM MG-132 (**C**) and 50 μM chloroquine (**D**) were added for the final 24 h and protein expression of α-SMA and calponin was tested using western blot. N=7. *p<0.05, **p<0.01 and ***p<0.001 (paired two tailed Student's t-test).

Role of AKAPs in regulating contractility and proliferation in human ASM strips

To investigate the functional consequence of increased contractile protein abundance that we observed in cultured ASM cells, we next incubated human ASM strips with st-Ht31 for 4 days then assessed methacholine-induced isometric contraction. Treatment with st-Ht31 significantly increased contraction as evidenced by the significant 1.3-fold increase in maximal force (E_{max}; Figure 5A).

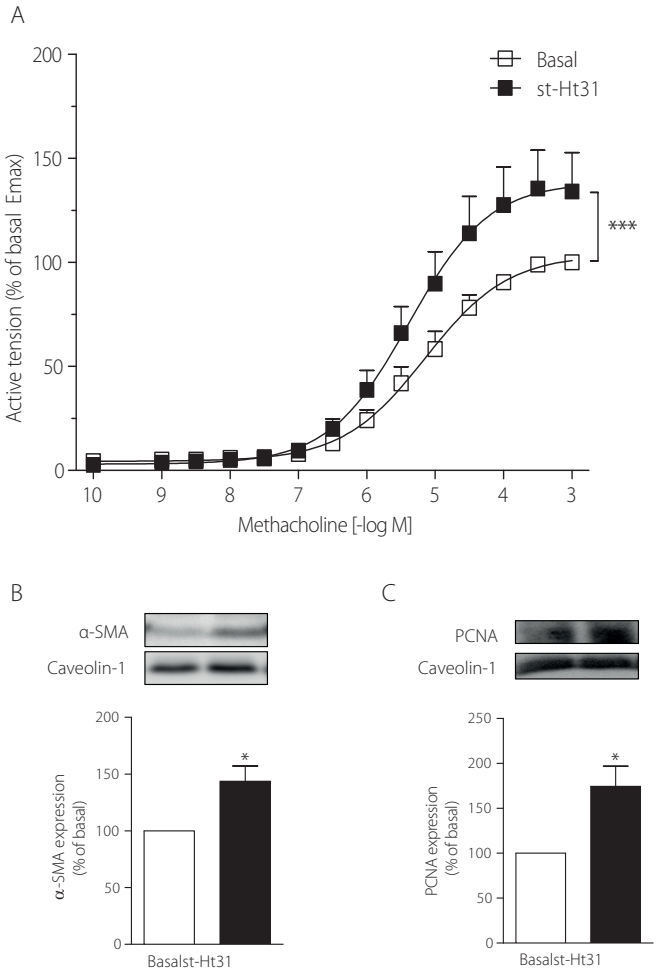

Figure 5. The effects of st-Ht31 on human tracheal strips. Isolated human tracheal strips were incubated with 50 μM st-Ht31 for 4 days. **A**: Methacholine-induced isometric contraction was measured. N=7-8. The expression of α-SMA (**B**) and PCNA (**C**) was determined in the tracheal strips. N=4-5, *p<0.05 (paired two tailed Student's t-test) and ***p<0.001 (extra sum-of-squares F test) compared to basal.

However, we did not observe any impact on sensitivity to methacholine (pD_2-values 5.28±0.18 and 5.36±0.18 for control and st-Ht31 treated, respectively). Notably, increased capacity to generate maximum force that was induced by st-Ht31 occurred with a concomitant increase in the abundance of α-SMA (Figure 5B). Interestingly, and in line with the findings in the cultured ASM cells that revealed st-Ht31-induced DNA synthesis, the abundance of PCNA was also increased by st-Ht31 treatment of human ASM tissue (Figure 5C).

Discussion

AKAPs are a group of structurally diverse proteins, which act as scaffolds for a variety of structural and signaling molecules, thereby facilitating effective targeting of different cellular microdomains (Wong and Scott 2004; Poppinga et al. 2014). As indicated by their name, all AKAPs combine with the regulatory subunits of PKA through a short α helical structure to guide activity in different sub-cellular locales (Esseltine and Scott 2013). This functional feature was exploited in development of the st-Ht31 peptide, as it mimics the short α helical structure in AKAPs to block their interaction with PKA (Vijayaraghavan et al. 1997). Since its development, st-Ht31 has been shown to alter a variety of cellular functions, including smooth muscle contraction and cell cycle progression (McConnell et al. 2009; Gao et al. 2012).

ASM cells exhibit phenotype plasticity, which allows modulation contractile and proliferative functional capacity in response to changes in the surrounding microenvironment (Halayko et al. 2008). Prolonged exposure to mitogens concomitantly induces a hyperproliferative ASM phenotype, characterized by increased DNA synthesis and mitosis, as well as a hypocontractile ASM phenotype, characterized by a reduced contractility and reduced contractile protein abundance (Halayko et al. 2008; Simeone-Penney et al. 2008; Roscioni et al. 2011a; Roscioni et al. 2011c). On the other hand, other stimuli such as insulin or changes in laminin isoform profile can induce a hypoproliferative and hypercontractile phenotype (Ma et al. 1998; Gosens et al. 2003; Schaafsma et al. 2007; Halayko et al. 2008; Dekkers et al. 2009). Interestingly, we now demonstrate that interruption of the interaction between PKA and AKAPs using st-Ht31 simultaneously increases markers of a hyperproliferative (*e.g.* DNA synthesis, activation of cell cycle proteins and increased expression of the proliferative marker PCNA) and a hypercontractile phenotype (*e.g.* increased expression of contractile proteins and increased contractility) in cultured ASM cells and in intact ASM strips.

Mitogen exposure of cells leads to phosphorylation and activation of p70S6K (Scott et al. 1996; Karpova et al. 1997; Grewe et al. 1999; Roscioni et al. 2011b), which promotes upregulation of the expression of a number of proteins, including cyclin D1 a critical cell cycle checkpoint determinant (Takuwa et al. 1999; Ravenhall et al. 2000; Chambard et al.

2007). We have demonstrated that p70S6K phosphorylation is reduced by activation of PKA (Roscioni et al. 2011a). Moreover, we have shown that PKA activity remains even after addition of st-Ht31 (Poppinga et al. 2015). Cyclin D1 can associate with pre-existing cyclin-dependent kinases to phosphorylate target proteins, such as Rb, that further enable and modulates cell cycle progress into S phase (Lundberg and Weinberg 1998). We now show that disruption of AKAP-PKA using st-Ht31 enables enhanced DNA synthesis. In line with this observation, st-Ht31 increased cyclin D expression as well as the phosphorylation of Rb and p70S6K, which have roles in regulating DNA synthesis progression (Withers et al. 1997; Takuwa et al. 1999). Furthermore, in intact ASM strips st-Ht31 treatment resulted in PCNA expression, a protein that is expressed during the S phase of the cell cycle (Leonardi et al. 1992). However, the increased DNA synthesis by st-Ht31 was not accompanied by an increase in cell number with prolonged treatment, suggesting that disruption of AKAP-ATP interaction is no sufficient in and of itself to induce cells to traverse S phase. In support, our FACS analysis in ASM cells showed that st-Ht31 had no significant impact on of the fraction of ASM cells in S phase. Taken together, these findings demonstrate that AKAP-PKA interaction is a modulator of early steps in DNA synthesis, likely by restraining the activation of p70S6K and expression of cyclin D1 and subsequent cell cycle proteins. In support, AKAPs, particularly AKAP8, interact with cyclins, including cyclin D1 (Eide et al. 1998; Arsenijevic et al. 2004; Qi et al. 2015; Han et al. 2015).

AKAP8 can reside in the nucleus, as confirmed by our studies, and is thought to be involved in DNA replication and expression of several genes associated with cell cycle regulation (Coghlan et al. 1994; Eide et al. 1998; Han et al. 2015). We now show that st-Ht31 reduced AKAP8 expression, with reduced protein in both the cytoplasm and the nucleus. On one hand, a AKAP8-cyclin D binding site has been identified that overlaps that for a CDK4 binding site, suggesting that nuclear AKAP8 may compete for cyclin D1 with CDK4 (Arsenijevic et al. 2006). Therefore, downregulation of AKAP8 with st-Ht31 could be permissive for interaction of cyclin D1 with CDK4, thereby supporting Rb phosphorylation and early S phase activities. On the other hand, AKAP8 has been found to regulate M phase events of the cell cycle such as chromatin condensation, by interacting with DNA and associated proteins such as a condensin complex component, Eg7 (Collas et al. 1999; Steen et al. 2000) and histone deacetylase 3 (HDAC3) (Li et al. 2006). Based on this, and in light of our observations, we hypothesize that, in addition to disrupting the interactions between AKAPs and PKA, st-Ht31-induced AKAP8 downregulation could contribute to disturbed cell cycle kinetics, that in our studies are revealed by increased proliferative markers but without increased cell number.

Besides inducing markers of a hyperproliferative phenotype in cultured ASM cells, st-Ht31 also increased the expression of the contractile proteins α-SMA and calponin, markers of a hypercontractile phenotype. An increase in α-SMA protein was also observed in intact

ASM strips treated with st-Ht31. An increased expression of contractile protein following 4 days treatment with st-Ht31 was also associated with an increased contractile response towards methacholine. Of note, the involvement of AKAPs has previously also been shown in isoprenaline-induced cardiac contraction (McConnell et al. 2009). As already noted, the proliferative marker protein PCNA was also increased in st-Ht31 treated ASM strips, supporting the notion that st-Ht31 simultaneously induces markers of a hyperproliferative as well as a hypercontractile phenotype.

In contrast to its effects on protein abundance, st-Ht31had little effect on mRNA for the calponin gene, *Cnn1,* and even decreased for abundance of mRNA from the α-SMA gene, *Acta2*. Therefore, the effects of st-Ht31 on α-SMA and calponin protein abundance appear to occur at a post-transcriptional or post-translational level. In support, the increase of α-SMA and calponin protein by st-Ht31 could not be prevented by blocking RNA synthesis using actinomycin D. Furthermore inhibition of protein translation using cycloheximide also did nto impact effects of st-Ht31. This suggests that st-Ht31 may affect protein stability, and indeed, AKAPs have recently been identified as factors involved in the ubiquitin-proteasome system (Rinaldi et al. 2015). Protein degradation via this system involves modification of the substrate protein by the covalent attachment of multiple ubiquitin molecules. The ubiquitin-tagged protein is eventually degraded through proteasomes (Ciechanover 2005). Using Co-IP we show that treatment with st-Ht31 increases ubiquitination of α-SMA protein, Nonetheless we also show that st-Ht31 also underpins accumulation of α-SMA protein, therefore, t-Ht31-induced ubiquitination of contractile proteins does not appear to lead to increased proteasomal degradation. This may suggest that st-Ht31 somehow inhibits proteasomal activity. In support, in our studies although basal abundance of calponin was increased by the proteasome inhibitor MG-132, it did not further increase the st-Ht31-induced accumulation of calponin. Furthermore, increased ubiquitination of proteins has also been observed by the proteasome inhibitor MG-132 itself (Ding et al. 2007). Currently, whether a ubiquitin-tagged contractile protein remains functional is unknown, which we think deserves further confirmation.

Taken together, treatment with st-Ht31 leads to a simultaneous increase in markers of a hypercontractile phenotype and those of a hyperproliferative phenotype in both ASM cells and intact strips. However, the increase in DNA synthesis and the activation of other cell cycle proteins (markers of a hyperproliferative phenotype) did not result in an increase in cell number. In contrast, the increase in contractile protein expression (marker of a hypercontractile phenotype) did lead to an increase in contractility, indicating the overall effect of disruption of AKAP-PKA interaction is the induction of a hypercontractile phenotype. Our observations could have major biological and drug development implications in obstructive respiratory disease, such as asthma and COPD, where there is both an increase in ASM mass and ASM contraction (Lambert et al. 1993; Chung 2005; Bentley and Hershenson

2008; Chung 2008). We recently demonstrated that the expression of several AKAPs in ASM and bronchial epithelial cells is differentially affected by cigarette smoke as well as in lung tissue of COPD patients (Oldenburger et al. 2014; Poppinga et al. 2015). In conclusion, AKAP-PKA interactions in ASM cells and intact ASM tissue simultaneously prevent the development of a hypercontractile phenotype, by restricting the expression of contractile proteins presumably by regulating proteasomal activity, as well as the development of a hyperproliferative phenotype, presumably by regulating the interaction of AKAP8 with cyclin D1.

Acknowledgments

B.H. was supported by a grant of the Ubbo Emmius Program of Faculty of Mathematics and Natural Sciences, University of Groningen; W.J.P. was supported by a grant from the Dutch Lung Foundation (3.2.11.15); M.S. was supported by a Rosalind Franklin Fellowship from the University of Groningen and a grant from the Deutsche Forschungsgemeinschaft (IRTG1874/1).

References

Akakura S, Huang C, Nelson PJ, et al (2008) Loss of the SSeCKS/Gravin/AKAP12 gene results in prostatic hyperplasia. Cancer Res 68:5096–5103. doi: 10.1158/0008-5472.CAN-07-5619

Amrani Y, Panettieri RA (2003) Airway smooth muscle: contraction and beyond. Int J Biochem Cell Biol 35:272–276. doi: 10.1016/S1357-2725(02)00259-5

Arsenijevic T, Degraef C, Dumont JE, et al (2004) A novel partner for D-type cyclins: protein kinase A-anchoring protein AKAP95. Biochem J 378:673–679. doi: 10.1042/BJ20031765

Arsenijevic T, Degraef C, Dumont JE, et al (2006) G1/S Cyclins interact with regulatory subunit of PKA via A-kinase anchoring protein, AKAP95. Cell Cycle Georget Tex 5:1217–1222. doi: 10.4161/cc.5.11.2802

Bentley JK, Hershenson MB (2008) Airway Smooth Muscle Growth in Asthma. Proc Am Thorac Soc 5:89–96. doi: 10.1513/pats.200705-063VS

Bertoli C, Skotheim JM, de Bruin RA (2013) Control of cell cycle transcription during G1 and S phases. Nat Rev Cell Biol 14:518–528. doi: 10.1038/nrm3629

Burgess A, Vigneron S, Brioudes E, et al (2010) Loss of human Greatwall results in G2 arrest and multiple mitotic defects due to deregulation of the cyclin B-Cdc2/PP2A balance. Proc Natl Acad Sci U S A 107:12564–12569. doi: 10.1073/pnas.0914191107

Chambard JC, Lefloch R, Pouyssegur J, Lenormand P (2007) ERK implication in cell cycle regulation. Biochim Biophys Acta 1773:1299–1310. doi: 10.1016/j.bbamcr.2006.11.010

Chung KF (2005) The role of airway smooth muscle in the pathogenesis of airway wall remodeling in chronic obstructive pulmonary disease. Proc Am Thorac Soc 2:347-54–2. doi: 2/4/347 [pii]

Chung KF (2008) Airway Smooth Muscle in Asthma and COPD: Biology and Pharmacology. John Wiley & Sons

Ciechanover A (2005) Proteolysis: from the lysosome to ubiquitin and the proteasome. Nat Rev Mol Cell Biol 6:79–87. doi: 10.1038/nrm1552

Coghlan VM, Langeberg LK, Fernandez A, et al (1994) Cloning and characterization of AKAP 95, a nuclear protein that associates with the regulatory subunit of type II cAMP-dependent protein kinase. J Biol Chem 269:7658–7665.

Collas P, Le Guellec K, Taskén K (1999) The A-kinase-anchoring protein AKAP95 is a multivalent protein with a key role in chromatin condensation at mitosis. J Cell Biol 147:1167–1180.

Dekkers BGJ, Schaafsma D, Tran T, et al (2009) Insulin-induced laminin expression promotes a hypercontractile airway smooth muscle phenotype. Am J Respir Cell Mol Biol 41:494–504. doi: 10.1165/rcmb.2008-0251OC

Dick FA, Rubin SM (2013) Molecular mechanisms underlying RB protein function. Nat Rev Cell Biol 14:297–306. doi: 10.1038/nrm3567

Ding W-X, Ni H-M, Gao W, et al (2007) Linking of autophagy to ubiquitin-proteasome system is important for the regulation of endoplasmic reticulum stress and cell viability. Am J Pathol 171:513–524. doi: 10.2353/ajpath.2007.070188

Eide T, Coghlan V, Orstavik S, et al (1998) Molecular cloning, chromosomal localization, and cell cycle-dependent subcellular distribution of the A-kinase anchoring protein, AKAP95. Exp Cell Res 238:305–316. doi: 10.1006/excr.1997.3855

Esseltine JL, Scott JD (2013) AKAP signaling complexes: pointing towards the next generation of therapeutic targets? Trends Pharmacol Sci 34:648–655. doi: 10.1016/j.tips.2013.10.005

Gao X, Chaturvedi D, Patel TB (2012) Localization and retention of p90 ribosomal S6 kinase 1 in the nucleus: implications for its function. Mol Biol Cell 23:503–515. doi: 10.1091/mbc.E11-07-0658

Gosens R, Nelemans SA, Hiemstra M, et al (2003) Insulin induces a hypercontractile airway smooth muscle phenotype. Eur J Pharmacol 481:125–131.

Gosens R, Stelmack GL, Dueck G, et al (2006) Role of caveolin-1 in p42/p44 MAP kinase activation and proliferation of human airway smooth muscle. Am J Physiol Cell Mol Physiol 291:L523-34. doi: 00013.2006 [pii]

Grewe M, Gansauge F, Schmid RM, et al (1999) Regulation of cell growth and cyclin D1 expression by the constitutively active FRAP-p70s6K pathway in human pancreatic cancer cells. Cancer Res 59:3581–3587.

Halayko AJ, Tran T, Gosens R (2008) Phenotype and functional plasticity of airway smooth muscle: role of caveolae and caveolins. Proc Am Thorac Soc 5:80–88. doi: 10.1513/pats.200705-057VS

Han B, Poppinga WJ, Schmidt M (2015) Scaffolding during the cell cycle by A-kinase anchoring proteins. Pflüg Arch - Eur J Physiol 1–11. doi: 10.1007/s00424-015-1718-0

Horvat SJ, Deshpande DA, Yan H, et al (2012) A-kinase anchoring proteins regulate compartmentalized cAMP signaling in airway smooth muscle. FASEB J Off Publ Fed Am Soc Exp Biol 26:3670–3679. doi: 10.1096/fj.11-201020

Karpova AY, Abe MK, Li J, et al (1997) MEK1 is required for PDGF-induced ERK activation and DNA synthesis in tracheal myocytes. Am J Physiol 272:L558-565.

Kim M, Kim M, Lee S, et al (2013) cAMP/PKA signalling reinforces the LATS-YAP pathway to fully suppress YAP in response to actin cytoskeletal changes. EMBO J 32:1543–1555. doi: 10.1038/emboj.2013.102

Kong J, Li Y, Liu S, et al (2013) High expression of ezrin predicts poor prognosis in uterine cervical cancer. BMC Cancer 13:520-2407-13–520. doi: 10.1186/1471-2407-13-520

Lambert RK, Wiggs BR, Kuwano K, et al (1993) Functional significance of increased airway smooth muscle in asthma and COPD. J Appl Physiol Bethesda Md 1985 74:2771–2781.

Leonardi E, Girlando S, Serio G, et al (1992) PCNA and Ki67 expression in breast carcinoma: correlations with clinical and biological variables. J Clin Pathol 45:416–419.

Li Y, Kao GD, Garcia BA, et al (2006) A novel histone deacetylase pathway regulates mitosis by modulating Aurora B kinase activity. Genes Dev 20:2566–2579. doi: 10.1101/gad.1455006

Lundberg AS, Weinberg RA (1998) Functional inactivation of the retinoblastoma protein requires sequential modification by at least two distinct cyclin-cdk complexes. Mol Cell Biol 18:753–761.

Ma X, Wang Y, Stephens NL (1998) Serum deprivation induces a unique hypercontractile phenotype of cultured smooth muscle cells. Am J Physiol 274:C1206-1214.

McConnell BK, Popovic Z, Mal N, et al (2009) Disruption of protein kinase A interaction with A-kinase-anchoring proteins in the heart in vivo: effects on cardiac contractility, protein kinase A phosphorylation, and troponin I proteolysis. J Biol Chem 284:1583–1592. doi: 10.1074/jbc.M806321200

Oldenburger A, Poppinga WJ, Kos F, et al (2014) A-kinase anchoring proteins contribute to loss of E-cadherin and bronchial epithelial barrier by cigarette smoke. Am J Physiol Physiol 306:C585-97. doi: 10.1152/ajpcell.00183.2013

Pawson T, Scott JD (1997) Signaling through scaffold, anchoring, and adaptor proteins. Science 278:2075–2080.

Pellagatti A, Cazzola M, Giagounidis A, et al (2010) Deregulated gene expression pathways in myelodysplastic syndrome hematopoietic stem cells. Leukemia 24:756–764. doi: 10.1038/leu.2010.31

Petrilli AM, Fernández-Valle C (2015) Role of Merlin/NF2 inactivation in tumor biology. Oncogene. doi: 10.1038/onc.2015.125

Poppinga WJ, Heijink IH, Holtzer LJ, et al (2015) A-kinase-anchoring proteins coordinate inflammatory responses to cigarette smoke in airway smooth muscle. Am J Physiol Cell Mol Physiol 308:L766-75. doi: 10.1152/ajplung.00301.2014

Poppinga WJ, Munoz-Llancao P, Gonzalez-Billault C, Schmidt M (2014) A-kinase anchoring proteins:

Cyclic AMP compartmentalization in neurodegenerative and obstructive pulmonary diseases. Br J Pharmacol. doi: 10.1111/bph.12882

Qi F, Yuan Y, Zhi X, et al (2015) Synergistic effects of AKAP95, Cyclin D1, Cyclin E1, and Cx43 in the development of rectal cancer. Int J Clin Exp Pathol 8:1666–1673.

Ravenhall C, Guida E, Harris T, et al (2000) The importance of ERK activity in the regulation of cyclin D1 levels and DNA synthesis in human cultured airway smooth muscle. Br J Pharmacol 131:17–28. doi: 10.1038/sj.bjp.0703454

Rinaldi L, Sepe M, Donne RD, Feliciello A (2015) A dynamic interface between ubiquitylation and cAMP signaling. Front Pharmacol 6:177. doi: 10.3389/fphar.2015.00177

Roscioni SS, Dekkers BG, Prins AG, et al (2011a) cAMP inhibits modulation of airway smooth muscle phenotype via the exchange protein activated by cAMP (Epac) and protein kinase A. Br J Pharmacol 162:193–209. doi: 10.1111/j.1476-5381.2010.01011.x

Roscioni SS, Maarsingh H, Elzinga CRS, et al (2011b) Epac as a novel effector of airway smooth muscle relaxation. J Cell Mol Med 15:1551–1563. doi: 10.1111/j.1582-4934.2010.01150.x

Roscioni SS, Prins AG, Elzinga CRS, et al (2011c) Protein kinase A and the exchange protein directly activated by cAMP (Epac) modulate phenotype plasticity in human airway smooth muscle. Br J Pharmacol 164:958–969. doi: 10.1111/j.1476-5381.2011.01354.x

Schaafsma D, McNeill KD, Stelmack GL, et al (2007) Insulin increases the expression of contractile phenotypic markers in airway smooth muscle. Am J Physiol Cell Physiol 293:C429-439. doi: 10.1152/ajpcell.00502.2006

Scott PH, Belham CM, al-Hafidh J, et al (1996) A regulatory role for cAMP in phosphatidylinositol 3-kinase/p70 ribosomal S6 kinase-mediated DNA synthesis in platelet-derived-growth-factor-stimulated bovine airway smooth-muscle cells. Biochem J 318 (Pt 3):965–971.

Simeone-Penney MC, Severgnini M, Rozo L, et al (2008) PDGF-induced human airway smooth muscle cell proliferation requires STAT3 and the small GTPase Rac1. Am J Physiol Lung Cell Mol Physiol 294:L698-704. doi: 10.1152/ajplung.00529.2007

Skroblin P, Grossmann S, Schafer G, et al (2010) Mechanisms of protein kinase A anchoring. Int Rev Cell Mol Biol 283:235–330. doi: 10.1016/S1937-6448(10)83005-9

Steen RL, Cubizolles F, Le Guellec K, Collas P (2000) A kinase-anchoring protein (AKAP)95 recruits human chromosome-associated protein (hCAP)-D2/Eg7 for chromosome condensation in mitotic extract. J Cell Biol 149:531–536.

Takuwa N, Fukui Y, Takuwa Y (1999) Cyclin D1 Expression Mediated by Phosphatidylinositol 3-Kinase through mTOR-p70S6K-Independent Signaling in Growth Factor-Stimulated NIH 3T3 Fibroblasts. Mol Cell Biol 19:1346–1358.

Vijayaraghavan S, Goueli SA, Davey MP, Carr DW (1997) Protein kinase A-anchoring inhibitor peptides arrest mammalian sperm motility. J Biol Chem 272:4747–4752.

Withers DJ, Seufferlein T, Mann D, et al (1997) Rapamycin Dissociates p70S6K Activation from DNA Synthesis Stimulated by Bombesin and Insulin in Swiss 3T3 Cells. J Biol Chem 272:2509–2514.

Wong W, Scott JD (2004) AKAP signalling complexes: focal points in space and time. Nat Rev Cell Biol 5:959–970. doi: 10.1038/nrm1527